Imaging extended reflectors in a terminating waveguide

C. Tsogka[2,3], **D. A. Mitsoudis**[1,3], **S. Papadimitropoulos**[2,3]

[1] Department of Energy Technology Engineering, Technological Educational Institute of Athens

[2] Department of Mathematics & Applied Mathematics, University of Crete

[3] Institute for Applied & Computational Mathematics, FO.R.T.H.

1. Setup

Goal: Image extended scatterers in a terminating waveguide.

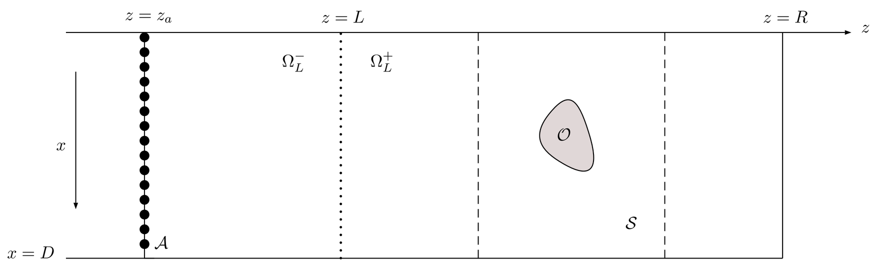

- Waveguide: Homogeneous in Ω_L^-, inhomogeneous in Ω_L^+.
- $\mathcal{O}$: extended scatterer (typical size $\sim$ wavelength, λ_0).
- vertical array $\mathcal{A}$: N transducers
- Data: Array response matrix $\widehat{\Pi}(\omega)$ for the scattered field.
- $\mathcal{S}$: search domain.

2. Preliminaries

The Helmholtz equation is given by

$$-\Delta\hat{p}^{\text{tot}}(\omega,\vec{x}) - k^2(\vec{x})\hat{p}^{\text{tot}}(\omega,\vec{x}) = \hat{f}(\omega,\vec{x}), \quad \vec{x}\in\Omega.$$

We denote $\widehat{G}^R(\vec{x},\vec{x}_s)$ the Green's function for the Helmholtz operator $-\Delta\cdot - k^2\cdot$, for a point source, where k is the (real) wavenumber. In Ω_L^- we denote $\{\mu_n, X_n\}_{n=1,2,\dots}$ the eigenpairs of

$$X''(x) + \mu X(x) = 0,\ x\in(0,D) \quad \text{and} \quad X(0)=X(D)=0,$$

and assume $\exists$ an index M such that it holds in Ω_L^-

$$\mu_M < k^2 < \mu_{M+1},$$

so we have the horizontal wavenumbers:

$$\beta_n = \begin{cases} \sqrt{k^2-\mu_n}, & 1\le n\le M, \ \rightsquigarrow \ \text{propagating modes} \\ \mathrm{i}\sqrt{\mu_n-k^2}, & n\ge M+1, \ \rightsquigarrow \ \text{evanescent modes} \end{cases}$$

3. Passive Imaging

We consider the passive imaging problem for a point source placed at $\vec{x}_s = (z_s, x_s)$.

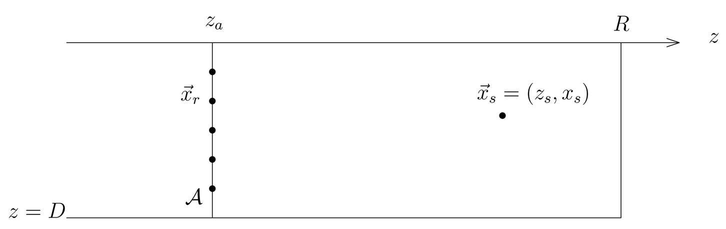

Our data for imaging is the vector $\widehat{\Pi}(\vec{x}_r,\omega)$,which is the Green's function going from $\vec{x}_s$ to $\vec{x}_r$:

$$\widehat{\Pi}(\vec{x}_r,\omega) = \widehat{G}^R(\vec{x}_r,\vec{x}_s,\omega).$$

Based on phase conjugation, we may write for a single frequency ω, $\vec{x}_r = (z_a, x)\in\mathcal{A}$ and $\vec{y}^s\in\mathcal{S}$:

$$\mathcal{I}^{PC}(\vec{y}^s) = \int_{\mathcal{A}} \overline{\widehat{G}^R(\vec{x}_s,\vec{x}_r)}\,\widehat{G}^R(\vec{x}_r,\vec{y}^s)\,dx,$$

If we assume that we have an array capable of recording the field as well as its normal derivative, then we have that

$$\mathcal{I}(\vec{y}^s) = \int_{\mathcal{A}} \left(\nabla\widehat{G}^R(\vec{x}_r,\vec{y}^s)\overline{\widehat{G}^R(\vec{x}_r,\vec{x}_s)} - \widehat{G}^R(\vec{x}_r,\vec{y}^s)\overline{\nabla\widehat{G}^R(\vec{x}_r,\vec{x}_s)}\right)\cdot dS.$$

where dS is the outward pointing surface element.
For our waveguide, we can prove a Kirhhoff-Helmholtz type identity [1], given by

$$\int_{\mathcal{A}} \left(\nabla\widehat{G}^R(\vec{y},\vec{y}^s)\overline{\widehat{G}^R(\vec{y},\vec{x}_s)} - \widehat{G}^R(\vec{y},\vec{y}^s)\overline{\nabla\widehat{G}^R(\vec{y},\vec{x}_s)}\right)\cdot dS = \widehat{G}^R(\vec{x}_s,\vec{y}^s) - \overline{\widehat{G}^R(\vec{x}_s,\vec{y}^s)},$$

which, after calculations can be written as

$$2i\sum_{n=1}^{M}\beta_n\overline{\widehat{G}_n^R(z_a,\vec{x}_s)}\,\widehat{G}_n^R(z_a,\vec{y}^s) = \widehat{G}^R(\vec{x}_s,\vec{y}^s) - \overline{\widehat{G}^R(\vec{x}_s,\vec{y}^s)},$$

where $\widehat{G}_n^R(z_a,\vec{x}_s)$ is the projection of the Green's function on the propagating modes,

$$\widehat{G}_n^R(z_a,\vec{x}_s) = \int_0^D \widehat{G}^R((z_a,x'),\vec{x}_s)\,X_n(x')\,dx'.$$

Let

$$\widehat{\mathbb{P}}_n = \int_0^D \widehat{\Pi}(\vec{x}_r,\omega)X_n(x)\,dx, \quad n=1\dots,M,$$

be the projection of the recorded field on the propagating modes [2]. In this case $\widehat{\mathbb{P}}_n$ is given by

$$\widehat{\mathbb{P}}_n = \int_0^D \widehat{G}^R((z_a,x),\vec{x}_s)X_n(x)\,dx \left(= \widehat{G}_n^R(z_a,\vec{x}_s)\right).$$

We define our imaging functional $\mathcal{I}^p$ as

$$\mathcal{I}^p(\vec{y}^s) := \sum_{n=1}^{M}\beta_n\overline{\widehat{\mathbb{P}}_n}\,\widehat{G}_n^R(z_a,\vec{y}^s).$$

From the Kirchhoff–Helmholtz identity we get

$$\mathcal{I}^p(\vec{y}^s) = \frac{1}{2i}\left(\widehat{G}^R(\vec{y}^s,\vec{x}_s) - \overline{\widehat{G}^R(\vec{y}^s,\vec{x}_s)}\right) = \operatorname{Im}\widehat{G}^R(\vec{y}^s,\vec{x}_s).$$

We consider a source located at $\vec{x}_s = (380,100)$ m and a single frequency $f=73$ Hz. The waveguide has depth $D=200$ m, $c_0=1500$ m/s. We have $M=19$ propagating modes, the vertical boundary is at $R=550$ m and our search domain is $\mathcal{S} = [230,530]\times[0,D]$.

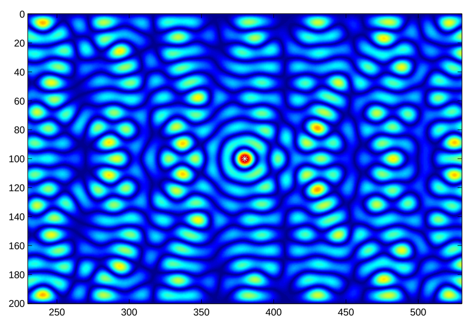

Good source localization

Low Signal-to-Noise Ratio (SNR)

4. Active Imaging

For a point scatterer, assuming unit reflectivity on the scatterer, the response matrix may be written as

$$\widehat{\Pi}(\vec{x}_s,\vec{x}_r,\omega) = \widehat{G}^R(\vec{x}^*,\vec{x}_s,\omega)\widehat{G}^R(\vec{x}_r,\vec{x}^*,\omega),$$

and the projected response matrix $\widehat{\mathbb{P}}$ is given by

$$\widehat{\mathbb{P}}_{nm} = \int_0^D\int_0^D \widehat{\Pi}(\vec{x}_s,\vec{x}_r,\omega)X_n(x_s)X_m(x_r)\,dx_s\,dx_r, \quad n=1\dots,M.$$

For active imaging we propose the use of

$$\mathcal{I}^a(\vec{y}^s) := \sum_{n=1}^{M}\sum_{m=1}^{M}\beta_n\beta_m\overline{\widehat{\mathbb{P}}_{nm}}\,\widehat{G}_n^R(z_a,\vec{y}^s)\,\widehat{G}_m^R(z_a,\vec{y}^s).$$

Using the Kirchhoff–Helmholtz identity we obtain

$$\mathcal{I}^a(\vec{y}^s) = \left(\operatorname{Im}\widehat{G}^R(\vec{y}^s,\vec{x}^*)\right)^2 = \left(\mathcal{I}^p(\vec{y}^s)\right)^2.$$

We consider a scatterer with the same setup as before.

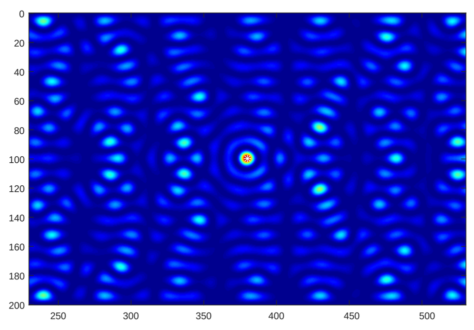

Good scatterer localization

Higher SNR than passive

5. Resolution analysis

For a homogeneous waveguide, $\mathcal{I}^p$ for $\vec{y} = (z,x)$, becomes

$$\mathcal{I}^p(\vec{y}) = \frac{1}{2}\sum_{n=1}^{M}\frac{1}{\beta_n}\left(\cos\beta_n(z-z_s) - \cos\beta_n(2R-z-z_s)\right)X_n(x)\,X_n(x_s).$$

We may consider it as a Riemann sum approximation of an integral which, in turn, can be evaluated analytically. Considering $\vec{y}$ at the correct range or cross-range, $\mathcal{I}^p$ becomes

$$\mathcal{I}^p(\vec{y}) \approx \frac{1}{16}\left[\left(J_0(\alpha_\ell) - J_0(\beta_\ell)\right) - \left(J_0(\sqrt{\alpha_\ell^2+\gamma_\ell^2}) - J_0(\sqrt{\beta_\ell^2+\gamma_\ell^2})\right)\right],$$

where for the cross-range, *i.e.* $\vec{y} = (z_s, x)$ and $\ell = x$,

$$\alpha_x = \frac{2\pi(x-x_s)}{\lambda}, \quad \beta_x = \frac{2\pi(x+x_s)}{\lambda}, \quad \gamma_x = \frac{4\pi}{\lambda}(R-z_s),$$

and for the range *i.e.* $\vec{y} = (z, x_s)$ and $\ell = z$,

$$\alpha_z = \frac{2\pi}{\lambda}(z-z_s), \quad \beta_z = \frac{2\pi}{\lambda}(2R-z-z_s), \quad \gamma_z = \frac{4\pi x_s}{\lambda}.$$

For $z_s \ll R$, the resolution is defined by $J_0(a)$, since a_x and a_z are much smaller than the other arguments.

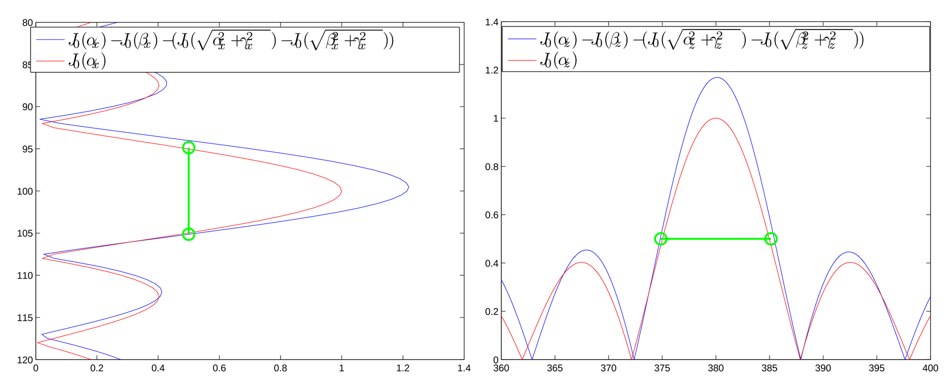

For both range and cross-range, the resolution is $\lambda_0/2$.

6. SNR issues

Our image has a widely varying SNR, for different frequencies.

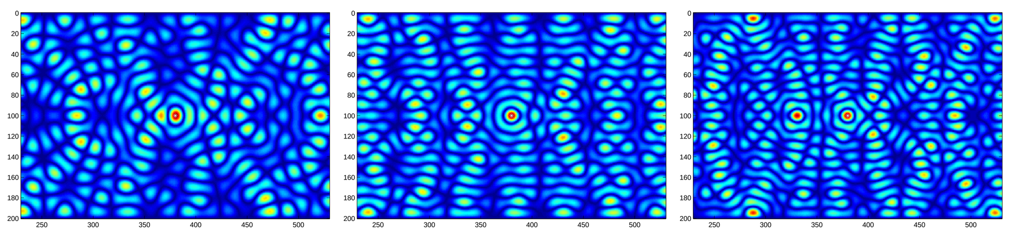

$f=65$ Hz $\quad f=73$ Hz $\quad f=81$ Hz

We wish to stabilize our image by using multiple frequencies.

1-D plots in depth (correct range)

Frequencies	Superimposed	Sum
$[67.625, 78.625]$ Hz, $B=11$ Hz		
$[31.875, 114.375]$ Hz, $B=82.5$ Hz		

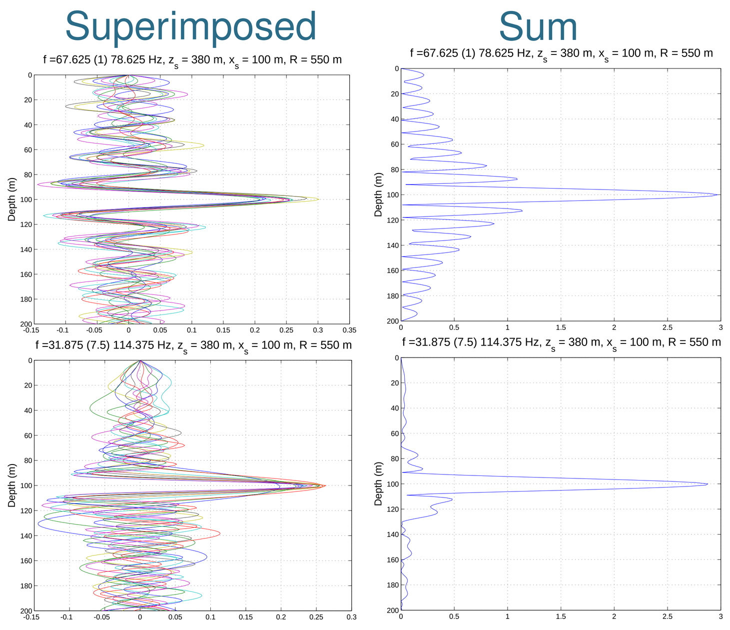

We observe coherent oscillations and high secondary peaks for the small bandwidth and incoherent oscillations and lower secondary peaks for the larger bandwidth. We have a similar behavior in range.

2-D plots

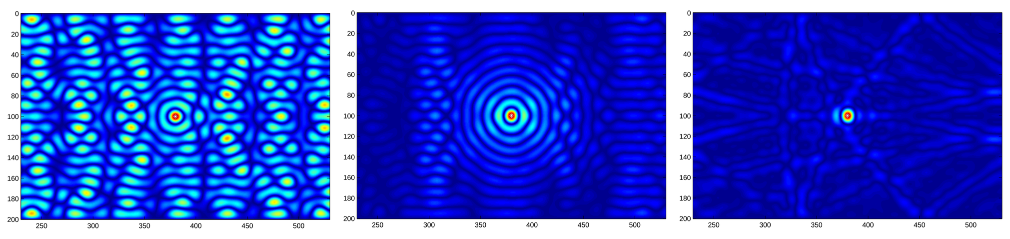

$f=73$ Hz $\quad f\in[67.625, 78.625]$ Hz, $B=11$ Hz $\quad f\in[31.875, 114.375]$ Hz, $B=82.5$ Hz

SNR improves as the bandwidth increases.

7. Extended scatterers

Semicircle (Data computed with Born)

Infinite — Terminating

No threshold

Threshold 0.4

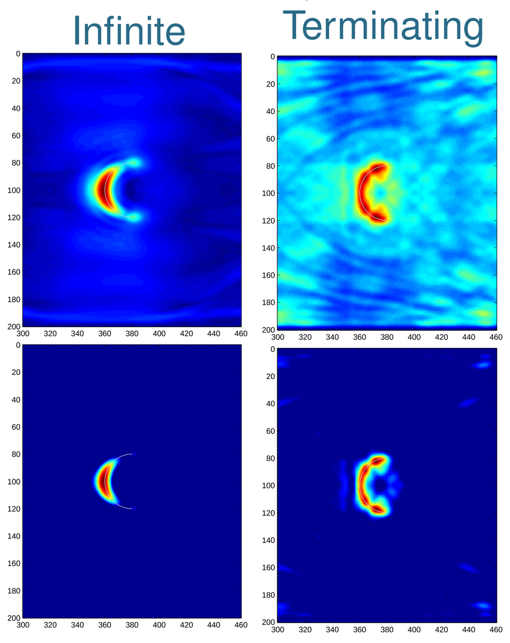

Disc (Data computed with Montjoie [3])

Infinite — Terminating

Threshold 0.4

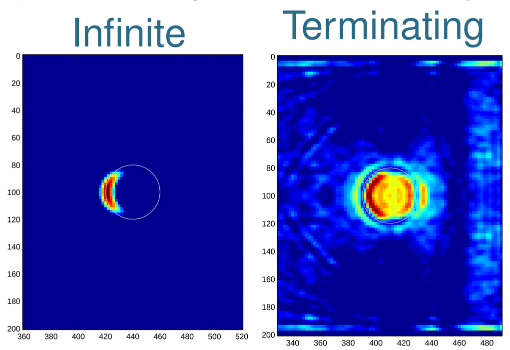

Rhombus (Data computed with Montjoie [3])

Infinite — Terminating

Threshold 0.4

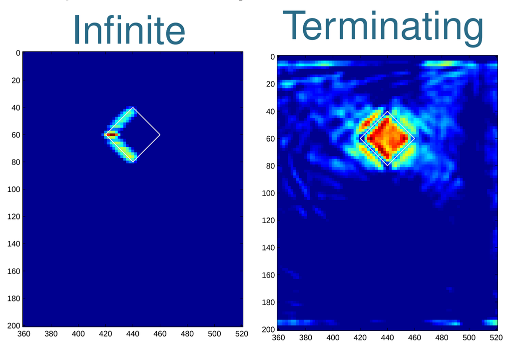

References

[1] D. Jackson, D. Dowling, *Phase conjugation in underwater acoustics*, JASA, 1991

[2] C. Tsogka, D.A. Mitsoudis, S.P., *Selective imaging of extended reflectors in two-dimensional waveguides*, SIAM J. Im. Sci., 2013

[3] Montjoie user's guide, *http:// montjoie.gforge.inria.fr*